



Solar nanophotocatalytic pretreatment of seawater: process optimization and performance evaluation using response surface methodology and genetic algorithm

Varghese Manappallil Joy¹ · Shaik Feroz² · Susmita Dutta¹

Received: 7 July 2020 / Accepted: 21 December 2020 / Published online: 14 January 2021
© The Author(s) 2021

Abstract

In reverse osmosis seawater treatment process, membrane fouling can be mitigated by degrading organic pollutants present in the feed seawater. The present study evaluates the effectiveness of employing solar photocatalysis using $\text{TiO}_2/\text{ZnO}/\text{H}_2\text{O}_2$ to pretreat reverse osmosis (RO) feed seawater under solar irradiation. Process optimisation and performance evaluation were undertaken using response surface methodology-desirability function and RSM integrated with genetic algorithm (RSM-GA). Statistical analysis was performed to determine the interactive relationships and main effects of input factors such as TiO_2 dosage, H_2O_2 dosage, pH, reaction time and ZnO dosage. The performance evaluation was determined in terms of percentage removal of total organic carbon (TOC) and chemical oxygen demand (COD). The obtained optimum values using RSM-GA evaluation for TOC and COD removal were found to be 76.5% and 63.9%, respectively. The predicted RSM-GA results correspond well with the experimental results (TOC removal = 73.3%, COD removal = 61.2%). Utilization of renewable solar energy coupled with optimum utilisation of nanophotocatalysts enables this technique to be a unique treatment process for RO pretreatment of seawater and membrane fouling mitigation.

Keywords Seawater pretreatment · Reverse osmosis (RO) membrane fouling · Solar nanophotocatalysis · Central composite design

Introduction

Seawater is becoming an increasingly significant water source globally due to high stress on freshwater availability and contamination issues. Based on lower installed capacity, seawater reverse osmosis (SWRO) surpasses all other thermal technologies like multi-stage flash (MSF) and multi-effect distillation (MED) and dominates the global desalination scenario. However, the performance of reverse osmosis (RO) membrane desalination systems majorly depends on fouling control and pretreatment processes to reduce contaminant loading (Amy et al. 2017). Fouling due to presence

of organics detrimentally affect the desalination systems by decreasing permeate flux, reducing energy efficiency due to high pressure drop and causing serious damage to the RO membranes (Weinrich et al. 2016). Many experimental studies revealed that the biofilm that affects membrane consists of around 50% organic matters, out of which about 40% are organic acids. RO membrane biofouling results in higher operating pressure, repeated chemical cleaning and reduces the life of the membrane (Matin et al. 2011).

Biofouling problem is very crucial in the Middle East region, where around 75% of RO membrane facilities are affected. Moreover, this is the region where the most considerable amount of desalted water is produced in the world (Khedr 2011). As per the literature survey, in most of the SWRO plants, humic substances (organic contaminants) are the main contributor of fouling to the RO membranes. If TOC of the seawater is less than 0.5 mg/L, the presence of microbial foulants is minimal, and the feed seawater has very low biofouling potential. For TOC values in the range of 0.5–2.0 mg/L, the RO feed seawater has moderate fouling potential. However, if the TOC exceeds 2.0 mg/L, the

✉ Susmita Dutta
susmita_che@yahoo.com

¹ Department of Chemical Engineering, National Institute of Technology Durgapur, Durgapur 713209, India

² Department of Mechanical Engineering and Deanship of Research, Prince Mohammad Bin Fahd University, Alkhobar, Kingdom of Saudi Arabia

biofouling potential is very high (Voutchkov 2017). Therefore, the deterioration of these contaminants from the RO feed seawater is a significant concern to improve the performance and cost-efficacy of SWRO systems. Advanced oxidation process with suitable photocatalysts can degrade persistent pollutants from the feed water. Remediation of recalcitrant pollutants is directly linked to the development of hydroxyl radicals (OH^\cdot) as it can degrade organic contaminants in the aquatic environment (Malato et al. 2016). Previous seawater decontamination studies revealed the advanced oxidation of recalcitrant pollutants by UV/photocatalysts methodology, where the processes either oxidised or entirely mineralised the model organic compounds. Rubio et al. (2013) evaluated the feasibility of disinfecting seawater by UV/ TiO_2 immobilized process. The study proved that TiO_2 photocatalysis has faster disinfection kinetics than UV alone for different bacterial disinfections. Jiménez et al. (2017) reported that the addition of TiO_2 accelerated the photo-Fenton process in treating cleaning waters from seawater desalination reverse osmosis membranes for recycling purposes.

Heterogeneous photocatalysis is an advanced oxidation technology capable of degrading a wide range of organic compounds present in the aquatic medium. Photocatalytic oxidation reactions have the potential to degrade the organic compounds to water and carbon dioxide and can provide clean and energy-saving technology for treating contaminated water. Due to solar irradiation, the photon having energy equal or greater than the semiconductor bandgap hits the catalyst to excite an electron from the valence band to the conduction band, resulting in the formation of electron-hole pair. These two entities are highly reactive and are involved in continuous oxidative and reductive reactions on semiconductor surface (Ab Aziz et al. 2016). As a result, hydroxyl radicals (OH^\cdot) are generated by the oxidation of H_2O or OH^- on the surface. The OH^\cdot radicals are highly powerful oxidants which can degrade recalcitrant organic pollutants from the medium. A typical semiconductor photocatalyst should be able to absorb near UV or visible light, chemically inert, photostable and inexpensive (Azevedo et al. 2009). Titanium dioxide (TiO_2) is a widely used semiconductor catalyst which shows promising characteristics even though in pure form, it gets activated only in UV region.

Although organic degradation of seawater by photocatalysis is comparatively lower due to electron scavenging issues, some of the past research studies showed very positive results in improving overall organic removal efficiency. Kaneva et al. (2015) studied the photocatalytic degradation of model organic in distilled and seawater by employing lanthanide modified ZnO under UV-light irradiation. It was observed that the photocatalyst achieves contaminant mineralization in minimum irradiation time. Ji et al. (2017) conducted a research study about photocatalytic removal

of diesel pollutants from seawater using $\text{ZrO}_2/\text{TiO}_2$ under visible light. In their work, photocatalyst effectiveness was investigated under the influence of various factors like doping ratio of catalyst, pH value, catalyst dosage, initial concentration of diesel and illumination time. They achieved 87.74% degradation of diesel pollutants from seawater under visible light photocatalysis. Many research studies enhanced the production rate of powerful oxidants by chemical addition, excitation energy (sunlight/UV), photocatalysts (TiO_2 , ZnO, Fe_2O_3 , CdS, ZnS) and combining two or more advanced oxidation process such as (TiO_2 /Fenton-UV), ozonation- TiO_2 and TiO_2 -Fenton-sunlight (Aljuboury et al. 2015). Yang et al. (2018) applied ZnO modified TiO_2 nanocomposites for organic pollutant removal from feedwater and reported enhanced degradation performance compared to pure TiO_2 . In the present study of seawater photocatalyst oxidation treatment, membrane fouling organic contaminants are degraded using TiO_2 -ZnO catalysts under solar irradiation.

Even though the semiconductor photocatalytic process is extensively employed in the treatment of effluents and other wastewater, little research studies were attempted in the field of pretreatment of RO desalination feed seawater. Several previous researchers applied photocatalytic technology for organics treatment from air, soil and wastewater, but very little work has been reported on seawater treatment, which may be due to the complexity of seawater composition. Optimization of TiO_2 -ZnO- H_2O_2 solar photocatalytic degradation of organics from seawater through DOE-based RSM-GA is still not available as per the knowledge of present research group concerned. This research paper presents for the first time, the application of RSM-GA optimization and solar nano ZnO- TiO_2 - H_2O_2 photocatalysis for the degradation of organics from seawater. The goal of this research study is to design and optimize a renewable energy-based photocatalytic process to mitigate RO membrane fouling in desalination plants.

The present study attempts to mitigate the fouling issues by photocatalytic degradation of organics and microorganism, using real seawater samples collected nearby a SWRO plant in Muscat, Oman. The current study evaluates the effectiveness of employing solar photocatalysis of $\text{TiO}_2/\text{ZnO}/\text{H}_2\text{O}_2$ process to pretreat RO feed seawater under solar irradiation. Process optimization and performance evaluation were undertaken using response surface methodology-desirability function (RSM-DF) and RSM integrated with genetic algorithm (RSM-GA) approach. Statistical analysis was performed to determine the interactive relationships and main effects of input factors such as TiO_2 dosage, H_2O_2 dosage, pH, reaction time (RT) and ZnO dosage. The performance evaluation was determined in terms of percentage removal of total organic carbon (TOC) and chemical oxygen demand (COD). Finally, the prediction accuracies of

optimum conditions by RSM-DF and RSM-GA techniques were compared, and the best solution is suggested for the overall process improvement in RO desalination seawater pretreatment.

Materials and methods

Materials and solar radiant flux measurement

Seawater sample, 2 km away from the shore, was collected in sterile bags and kept in the freezer (5 °C) until it was taken for solar photocatalytic treatment. The samples were characterized before the treatment to determine COD and TOC. The catalysts used were nano zinc oxide (ZnO, 99.9% Pure, APS: 20 nm), obtained from mkNANO, Canada and titanium dioxide (TiO₂) Aeroxide P-25 manufactured by Evonik Industries, Germany and 0.1 N of NaOH and HCl of 0.1 N were used for adjusting pH. COD test was done by using COD HR+ (0–15,000 mL/L) reagent vial from CHEMetrics, COD digester and COD HR photometer. TOC of each sample was determined by using TOC analyser (LCSH/CSN) supplied by SHIMADZU, Japan. Before analyzing TOC and COD, each sample was filtered using 0.22 μm Millipore Durapore membrane (150 mm-diameter and ashless-40).

The silt density index (SDI) of the seawater sample before and after photocatalytic treatment was calculated using SDI kit (SDI-2000, directSDI, 115–120 v, 60 Hz, USA). The average solar radiant flux was measured using KIPP & ZONEN-CMP 21 Pyranometer and found to be approximately 670 W/m². All experimental runs were carried out from 11 a.m. to 2 p.m. so that maximum UV radiation was received for photocatalytic treatment. The UVS-E-T radiometer supplied by KIPP & ZONEN was used to measure UV irradiance as per ISO 17166:1999, CIE S 007/E-1998 procedure. UV irradiance was determined by using Eq. 1.

$$I_{\text{solar}} = E/C_s \quad (1)$$

where C_s is the radiometer sensitivity constant ((μV/W)/m²), E (μV) is the voltage output, and I_{solar} (W/m²) is the solar irradiance.

Experimental procedure

The experimental setup of TiO₂/ZnO/H₂O₂/solar nano-photocatalytic reactor system is shown in Fig. 1. Five borosilicate glass tubes (650 mm length × 22 mm inner diameter and 2 mm thickness) were used for seawater recirculation exposed to solar irradiation. The setup consists of a glass recirculation tank (2.5 L) subjected to stirring with magnetic stirrers. Seawater solution was run through the tubular photocatalytic reactor by means of a peristaltic pump (PERCOM

N-M-II Peristaltic pump, 0.5–350 rpm, 0–2100 mL/min, 48 Watts) at a flow rate of 1.8 L per minute. The flow rate was fixed constant for all experimental runs. The pH of the solution was varied from 2 to 8 as per the factor settings of each run, prescribed by one-factor-at-a-time (OFAT) study and the central composite design (CCD) matrix. Samples were taken for TOC and COD analysis at respective reaction time interval settings, which was varied from 30 to 210 min. The tilt of the reactor was fabricated (19°–24° angle with horizontal) to make it align with solar angle and was conformable to the location latitude (23° 40' 12.97" N). Parabolic reflectors were installed beneath the reactor tubes to make the solar irradiation to be reflected and diffused to the tubes at optimum intensity. The magnetic stirring, aeration using an air pump (4.29 L/min) and recirculation using peristaltic pump ensured proper mixing and enough supply of oxygen required for photocatalytic reaction. The aeration process and the resulting air bubbles acted as a source of oxygen to enhance the overall photocatalytic degradation rate (Tony et al. 2009). The post-separation of the catalysts is accomplished by overnight settling process in a sedimentation tank. Since the pH of the seawater reaches near to the point of zero charge (pH_{PZC}) after the photocatalytic treatment, the catalyst surface charge neutralisation improves the sedimentation and aggregation process.

Effect of operating variables on TOC and COD removal

The initial concentration of TOC of seawater samples used in this experimental study is found to be less than 3.89 mg/L. In seawater reverse osmosis (SWRO) plants, an increase in initial TOC value beyond a threshold value (2.0–2.5 mg/L) is found to elevate enhanced biofouling of RO membranes. Hence, the main objective of this research study is to reduce the biofouling potential of seawater by degrading the TOC level well below the critical value of 2.0 mg/L. To evaluate the effect of input variables on the percentage removal of TOC and COD, variables such as TiO₂ dosage (0.1–0.8 g/L), ZnO dosage (0.1–0.8 g/L), H₂O₂ dosage (0.2–1.0 mL/L), solar irradiation time (30–210 min) and pH (2–8) were varied sensibly during the photocatalytic reactions. For the initial range finding and screening, one-factor-at-a-time (OFAT) experimental design was followed. OFAT enables to detect more quickly if a factor has any effect on the response variable of interest and is, therefore, a sequential learning methodology (Sen et al. 2017). Among the five input factors, at first, the effect of TiO₂ dosage was investigated. ZnO dosage, H₂O₂ dosage, solar irradiation time and pH were kept constant at 0.5 g/L, 0.5 mL/L, 180 min and 8, respectively. In the second stage, to identify the effect of ZnO dosage on percentage removal of TOC and COD, it was varied from 0.1 to 0.8 g/L, keeping v dosage, solar irradiation time and

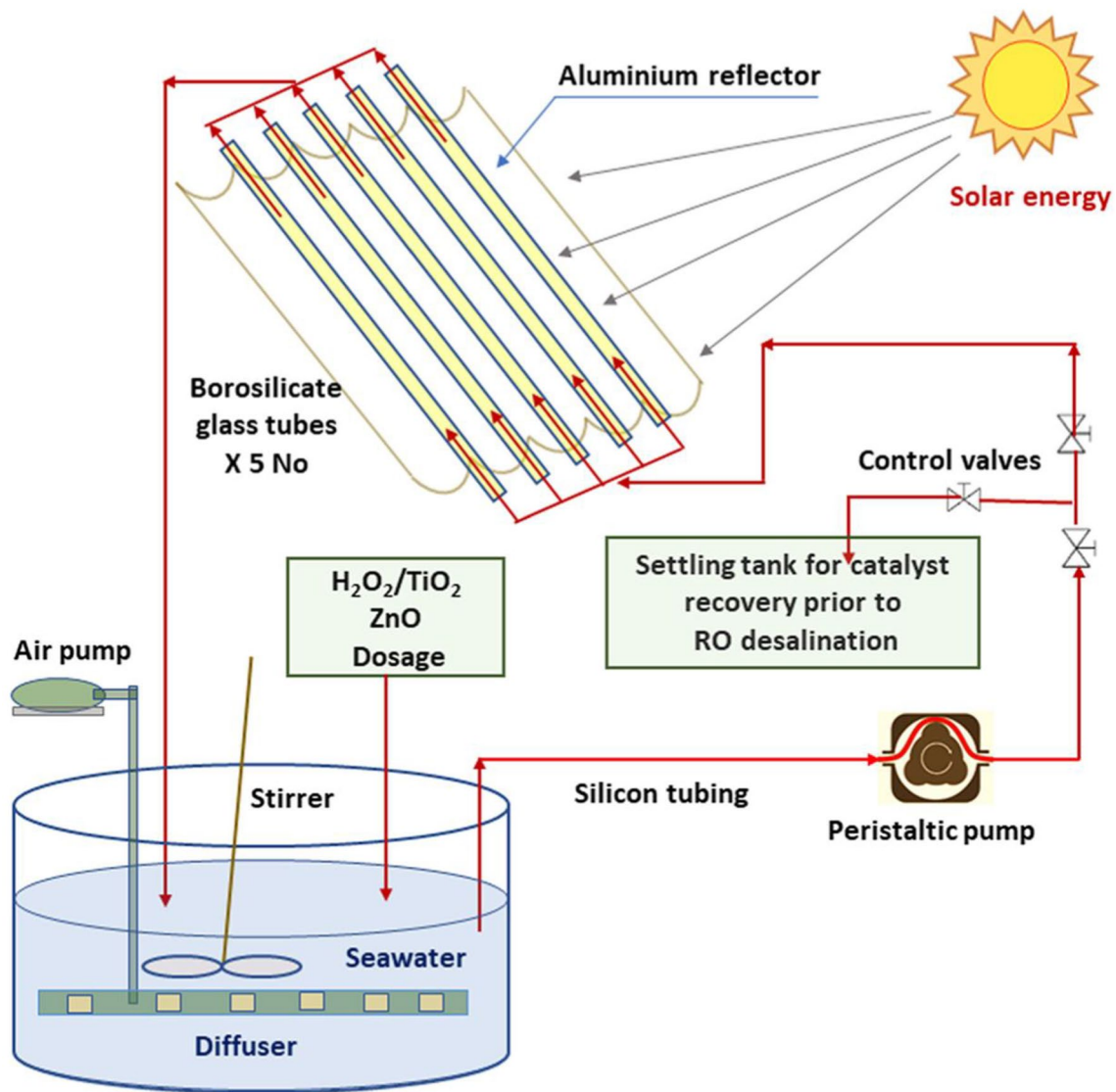


Fig. 1 Experimental setup of Solar/TiO₂/ZnO/H₂O₂ photocatalytic reactor system

pH at 0.5 mL/L, 180 min and 8, respectively. However, the TiO₂ dosage which gave the best result in the initial OFAT experiments was selected for the current set of experiments. Similarly, H₂O₂ dosage, irradiation time and pH were varied in the range of 0.2–1.0 mL/L, 30–210 min and 2–8, respectively, keeping other input factors constant at the values in which they gave best TOC and COD removal. The results from OFAT study were used to find the levels of input variables.

TOC and COD removal (%) were calculated by using Eqs. 2 and 3, respectively.

$$\text{TOC}_{\text{removal}} (\%) = \frac{T_0 - T_t}{T_0} \times 100 \quad (2)$$

where T_0 is the initial TOC of seawater before treatment and T_t represents the total organic carbon content after “ t ” minutes of solar irradiation.

$$\text{COD}_{\text{removal}} (\%) = \frac{C_0 - C_t}{C_0} \times 100 \quad (3)$$

where C_0 is the initial COD of seawater before photocatalytic treatment and C_t represents the chemical oxygen demand after “ t ” minutes of solar irradiation.

Design of experiments and statistical analysis

DOE-based response surface methodology (RSM) was used for experimental design and process optimization

with Design-Expert (version 11, Stat-Ease, USA) software. Response surface methodology is a statistical tool utilising experimental data generated from the respective design to optimize and model any system in which the response variable under study is affected by crucial input factors (Chatterjee et al. 2012). RSM is a competent technique for process optimization, strategically computing optimum condition for a multivariate process. This technique helps to establish relationships between response variables and controllable input variables or process factor, but the main limitation of this technique is that it can assume only nonlinear quadratic correlation and therefore requires a narrow search window (Desai et al. 2008), finding which requires either new OFAT experiments or good prior knowledge of the system. Central composite design (CCD) is a typical RSM technique well suited for fitting a second-order curve and optimizing significant process parameters that influence the dependent variables.

The efficiency of the photocatalytic treatment is analysed in term of percentage removal of COD and TOC by conducting experimental runs through a CCD matrix. Each independent process factor is varied between coded -1 (low), 0 (centre) and $+1$ (high) levels at predetermined ranges calculated from the preliminary OFAT experimentation. CCD-RSM model was generated using data from 48 experimental runs ($=2^n + 2n + n_c$, where n is the number of factors which is equal to 5). Thus, CCD in this research work consists of 2^n factorial runs augmented with $2n$ axial experiments, and n_c is the number of central runs. The central runs are used as replications to evaluate the reproducibility of the data and experimental errors. The sequence of experimental runs is randomized to avoid random process variations. The outcome from each run was tabulated into the Design-Expert software to correlate the responses with input factors. The second-degree polynomial equation for a response that explains its behaviour is shown in Eq. 4. Since each input factor is set at three levels, the appropriate model for the response follows a quadratic model.

$$Y = \beta_0 + \sum_{j=1}^k \beta_j X_j + \sum_{j=1}^k \beta_{jj} X_j^2 + \sum_{j<l}^k \beta_{jl} X_j X_l + e_i \quad (4)$$

where Y is the response forecasted, β_0 is the regression coefficient, β_j is the coefficient of linearity, β_{jj} is the coefficient of interaction, and β_{jl} is the quadratic coefficient, X_i and X_j are input variables, k represents the number of input factors, and e_i denotes random process error. After generating a quadratic RSM model, its input space is optimized using desirability function (DF) method. The optimal solution from RSM-DF is again compared by using RSM integrated genetic algorithm (GA) approach.

Genetic algorithm (GA), an artificial intelligence-based stochastic nonlinear optimization method, can be used to

optimize the input space of any well-trained models like artificial neural network (ANN) model (Dibaba et al. 2016). While GA may be used to configure optimum ANN model, the same ANN model, or any RSM model, can be used as an objective (fitness) function within GA to generate optimum function values and process settings (Sharma et al. 2017; Kumar and Kumar 2019). After the development of a generalized ANN or RSM model, the GA approach is used to find the optimum process settings. Therefore, GA is an optimization strategy developed based on the principles of natural selection that start with the selection of fittest individuals from a population (Mukherjee et al. 2019). A solution of GA is characterized by a chromosome having a fitness value which ensures the solution to be competent enough. The parameters of GA may comprise of a set of the population consist of chromosomes and genes, selection, crossover, mutation, fitness and fitness function (Abdollahi et al. 2019). The algorithm begins with a random initial set of population and a selection process based on fitness value to create the next generation. Crossover and mutation principles are used to combine genes for the next iteration and apply stochastic changes to reproduce population (Hassani et al. 2018). Upon the successive generations, the population evolves, and the optimum solution is determined. In the current study, the optimum solution obtained from RSM-GA simulation is compared with RSM optimal conditions generated by Design-Expert software.

Results and discussion

Characterization of seawater

The seawater sample, collected from Muscat, Gulf of Oman, was characterized in terms of total organic carbon (TOC), pH, salinity, etc. Table 1 summarizes the physicochemical characteristics of the sample seawater collected before

Table 1 Characteristics of seawater sample from the Gulf of Oman, 2.0 km away from the shore, at the location 23° 41.921' N, 058° 11.115' E

No	Parameter	Unit	Range of concentrations in seawater
1	Ph	–	7.5–8.1
2	Conductivity	mS	52.34–56.22
3	Salinity	mg/L	34,000–34,400
4	Turbidity	NTU	1.50–1.65
5	Dissolved oxygen, DO	mg/L	5.12–5.38
6	Total dissolved solids, TDS	mg/L	53,200–53,400
7	Chemical oxygen demand, COD	mg/L	4.9–5.78
8	Total organic carbon TOC	mg/L	2.94–3.89

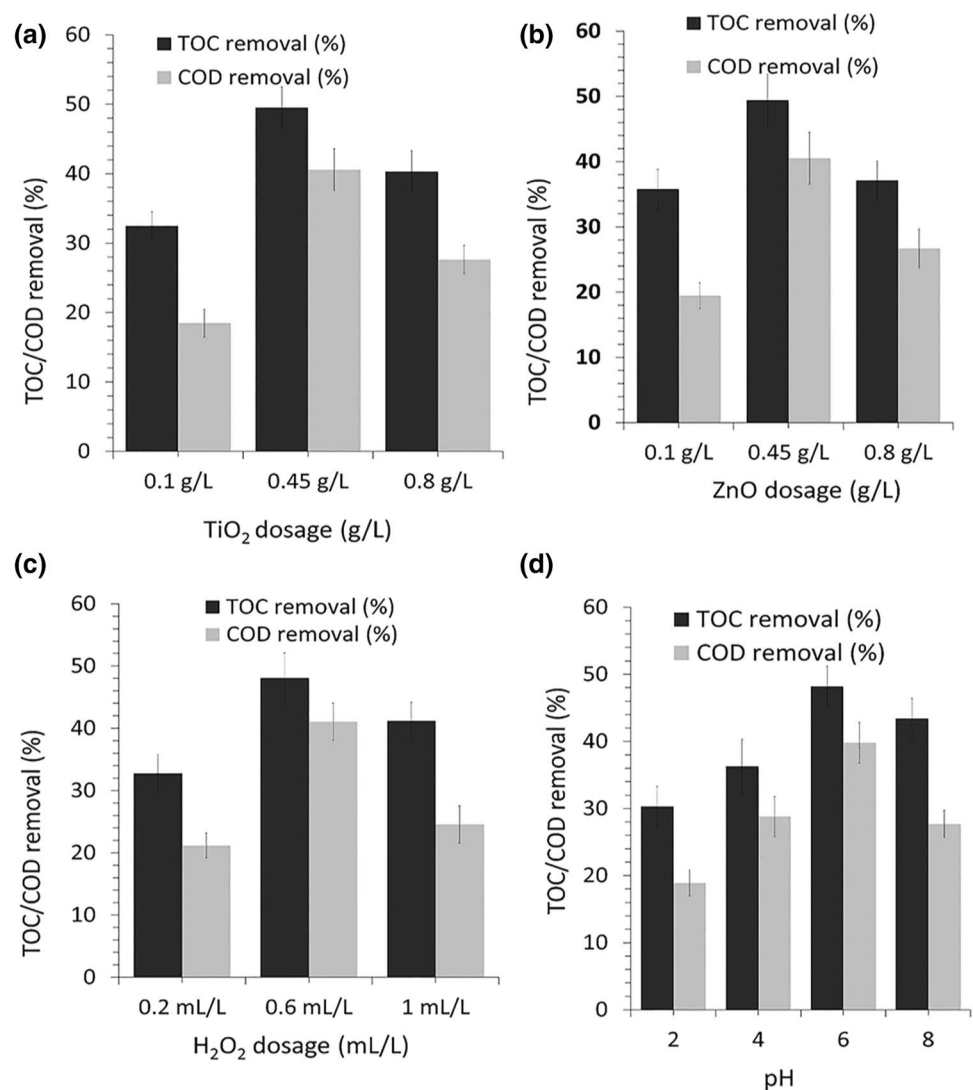
each experiment. The silt density index (SDI) of the seawater samples before and after photocatalytic treatment (under optimum conditions) is found to be 0.45 and 0.38, respectively.

Effect of process input factors on the removal of TOC and COD

For determining the significance and optimum ranges of operating variables, OFAT study has been conducted by judiciously varying one input factor at a time while keeping other factors at constant levels. At first, TiO_2 dosage has been varied in the range of 0.1–0.8 g/L, while ZnO dosage, H_2O_2 dosage, solar irradiation time and pH were kept constant at 0.5 g/L, 0.5 mL/L, 180 min and 8, respectively. The TOC and COD removal have been measured after each photocatalytic reactions, as shown in Fig. 2a. It was observed that maximum TOC removal ($49.5 \pm 4.25\%$)

and COD removal ($40.5 \pm 4.12\%$) occurred at TiO_2 dosage of 0.45 g/L and higher dosages resulted in reduced organic removal efficiency. Similar results were obtained with ZnO dosage (Fig. 2b). In a previous study to remove organics from petroleum wastewater, Dheea et al. observed a similar trend at higher concentrations of TiO_2 and ZnO catalysts (Aljuboury et al. 2016). Turbidity caused by a higher concentration of catalysts hinders the penetration of light into the reactor and hence reduced organic removal efficiency is observed (Malato et al. 2009). In the current study, the values of TiO_2 and ZnO dosages obtained from first two sets of experiments were used in the third OFAT study where maximum removal (TOC removal = $48.1 \pm 4.15\%$, COD removal = $41.8 \pm 3.84\%$) is achieved at H_2O_2 dosage of 0.6 mL/L (Fig. 2c). Generally, the degradation efficiency increases with H_2O_2 dosage in the initial phase of the photocatalytic reaction. However, after an optimal threshold value, a further increase in H_2O_2 concentration inversely

Fig. 2 a TOC removal (%) and COD removal (%) at ZnO dosage 0.5 g/L, H_2O_2 dosage 0.5 mL/L, solar irradiation time 180 min and pH 8 for different TiO_2 dosage; b TOC removal (%) and COD removal (%) at TiO_2 dosage 0.45 g/L, H_2O_2 dosage 0.5 mL/L, solar irradiation time 180 min and pH 8 for different ZnO dosage; c TOC removal (%) and COD removal (%) at TiO_2 dosage 0.45 g/L, ZnO dosage 0.45 g/L, solar irradiation time 180 min and pH 8 for different H_2O_2 dosage; d TOC removal (%) and COD removal (%) at TiO_2 dosage 0.45 g/L, ZnO dosage 0.45 g/L, H_2O_2 dosage 0.6 mL/L, solar irradiation time 180 min for different pH



affects organic degradation due to the distinct nature of H_2O_2 as a radical scavenger. In the fourth sets of experiments, pH was varied from 2 to 8 (Fig. 2d) where maximum organic degradation (TOC removal = $48.3 \pm 3.32\%$, COD removal = $39.9 \pm 3.45\%$) was achieved at pH 6, TiO_2 dosage 0.45 g/L, ZnO dosage 0.45 g/L, H_2O_2 dosage 0.6 mL/L and solar irradiation time of 180 min. At acidic operational pH, the surface charge for TiO_2 becomes positive and exerts an attractive electrostatic force on anionic organic composites which in turn enhances the photocatalytic degradation. Figure 3 shows TOC removal and COD removal at TiO_2 dosage 0.45 g/L, ZnO dosage 0.45 g/L, H_2O_2 dosage 0.6 mL/L and pH 6 for different solar irradiation time. It was found that maximum TOC removal ($48.2 \pm 2.75\%$) and COD removal ($40.7 \pm 3.13\%$) occurred at a solar reaction time (RT) of 150 min and further increment in time does not give any improvement in organic removal efficiency. Since the irradiation time depends on the initial concentration and ionic state of various organic contaminants, after a certain threshold, the degradation rate remains unchanged.

Five-factor centre composite design (CCD)

The results obtained from the OFAT study was utilized in identifying the design space and fixing the operating ranges of input parameters in CCD-RSM-DF modelling and optimization process. In RSM modelling, TiO_2 dosage, ZnO dosage, H_2O_2 dosage, reaction time (RT) and pH were chosen as input parameters, and the coded +1 (high) level and -1 (low) level were set at 0.2 and 0.7 g/L, 0.2 and 0.7 g/L, 0.3 and 0.9 mL/L, 60 and 180 min and 3 and 7, respectively. Table 2 shows the central composite design

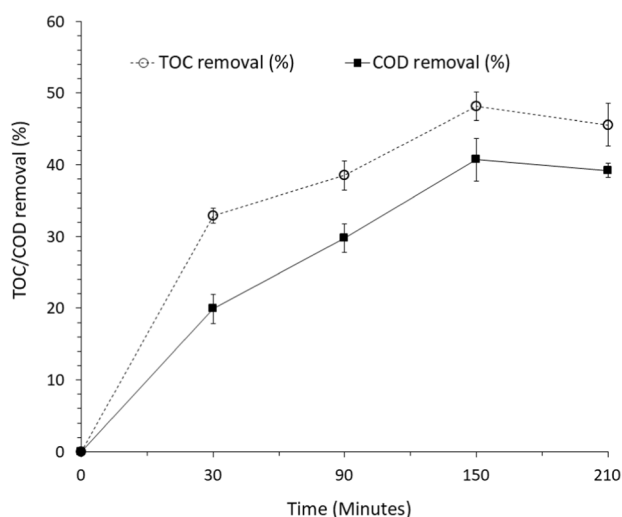


Fig. 3 TOC removal (%) and COD removal (%) at TiO_2 dosage 0.45 g/L, ZnO dosage 0.45 g/L, H_2O_2 dosage 0.6 mL/L and pH 6 for different solar irradiation time

layout and the respective response values generated from each experimental run. The COD removal ranges from 13.6 to 56.9%, while the TOC removal lies between 27.1% to a maximum of 67.3%.

Analysis of variance (ANOVA) study

In the present study, ANOVA was used for statistical analysis of the data to determine main and interaction effects between input factors and process responses. Tables 3 and 4 show the ANOVA modelling parameters for response-surface generated second-order model for TOC removal and COD removal, respectively. Influence of independent variables on each response is demonstrated in these tables. All the insignificant terms (except the terms for hierarchy) with a p value greater than 0.05 have been removed from the model. Lack of fit test checks whether the regression model fits well or not and compares the variation that is visible in the replicates with the variation present in the model. Significance of polynomial model terms and the model was assessed by the p value (probability) with a 95% confidence level. Models with good fit should have R^2 value greater than 0.8. In the present research, the predicted R^2 value for TOC and COD degradation was found to be 0.92 and 0.91, respectively. The R^2 determines the amount of correlation between the predicted responses and experimental data. Large R^2 value (nearing 1) demonstrates decent agreement between the observed and calculated results.

The adequate precision (AP) fractions of COD and TOC response models in this study were found to be 64.3 and 53.4, respectively. This ratio measures the signal-to-noise ratio to estimate the validity of the regression models obtained. AP values above four are required to qualify the models to be used for process optimization and navigate the design space formulated by the central composite design (CCD). As per ANOVA results, COD and TOC models were found significant by F test at 95% confidence level (Prob < 0.05). The response model F -ratio of 209.2 and 322.7 with low probability values ((Prob > F) < 0.05) shows that both models are significant enough to predict the response and optimum values. The difference between adjusted and predicted R^2 should be within 0.2, which was satisfied with both models.

CCD models in terms of actual and coded factors

Table 5 shows CCD equations of TOC and COD removal (%) in coded and actual factor terms. Coded factor models provide more meaningful insight about the process than equations represented in terms of actual factors. In coded factors, the terms are normalized and depicted in relative weights, while in equations with actual factors, owing to the presence of units, the prominence of coefficients is

Table 2 Five-factor central composite design (CCD) matrix; input factors at actual levels and the corresponding experimental and predicted results

Run	Input factors					Experimental		RSM-predicted	
	A: TiO ₂ (g/L)	B: ZnO (g/L)	C: H ₂ O ₂ (mL/L)	D: pH	E: RT (min)	TOC removal (%)	COD removal (%)	TOC removal (%)	COD removal (%)
1	0.45	0.45	0.3	5	120	60.2	41.6	56.31	40.75
2	0.45	0.45	0.6	5	120	61.1	53.9	60.50	50.97
3	0.2	0.2	0.9	7	180	59.5	33.6	57.98	33.23
4	0.7	0.7	0.9	3	60	44.8	34.6	42.39	33.29
5	0.45	0.7	0.6	5	120	53.1	50.2	54.16	50.86
6	0.2	0.7	0.9	7	180	62.2	37.2	59.35	37.49
7	0.45	0.45	0.6	7	120	67.3	56.9	67.03	55.39
8	0.7	0.2	0.9	7	180	62.1	37.9	64.32	37.98
9	0.2	0.7	0.9	3	180	42.5	27.2	44.14	28.63
10	0.45	0.45	0.6	5	60	57.1	43.7	56.46	42.46
11	0.2	0.7	0.3	7	60	39.5	26.3	39.26	26.58
12	0.7	0.2	0.9	3	60	41.9	23.8	41.03	23.07
13	0.7	0.7	0.9	3	180	50.1	39.6	50.48	39.35
14	0.2	0.2	0.3	7	180	42.2	29.9	45.99	28.38
15	0.7	0.7	0.3	3	60	36.7	30.5	37.62	31.35
16	0.7	0.2	0.3	7	60	47.2	30.1	47.17	29.98
17	0.2	0.7	0.3	3	180	36.3	22.9	36.44	23.78
18	0.45	0.45	0.6	3	120	54.2	46.7	53.97	46.54
19	0.45	0.2	0.6	5	120	52.2	44.2	52.79	43.62
20	0.7	0.2	0.3	7	180	57.3	36.3	55.26	36.04
21	0.2	0.7	0.3	3	60	29.1	18.7	28.35	17.72
22	0.7	0.7	0.3	3	180	43.6	37.4	45.71	37.41
23	0.7	0.45	0.6	5	120	56.2	51.2	56.93	51.39
24	0.45	0.45	0.6	5	120	57.1	48.1	60.50	50.97
25	0.7	0.2	0.9	7	60	56.5	32.4	56.23	31.92
26	0.2	0.2	0.3	3	60	27.1	13.6	26.98	13.46
27	0.2	0.2	0.9	3	60	34.3	17.7	34.69	18.31
28	0.2	0.2	0.3	3	180	35.3	19.9	35.07	19.52
29	0.45	0.45	0.6	5	180	65.5	47.2	64.55	48.52
30	0.2	0.2	0.3	7	60	38.5	20.3	37.90	22.32
31	0.2	0.2	0.9	3	180	44.2	25.8	42.78	24.37
32	0.2	0.7	0.9	3	60	35.3	23.6	36.05	22.57
33	0.45	0.45	0.9	5	120	64.2	45.2	64.70	45.14
34	0.2	0.7	0.3	7	180	48.7	32.8	47.35	32.64
35	0.7	0.2	0.3	3	180	44.3	28.5	44.35	27.19
36	0.7	0.7	0.3	7	180	56.8	47.2	56.63	46.26
37	0.45	0.45	0.6	5	120	61.4	49.2	60.50	50.97
38	0.45	0.45	0.6	5	120	58.5	52.5	60.50	50.97
39	0.2	0.2	0.9	7	60	48.4	25.6	49.89	27.17
40	0.2	0.7	0.9	7	60	51.3	32.4	51.26	31.43
41	0.2	0.45	0.6	5	120	48.2	42.3	49.12	42.20
42	0.45	0.45	0.6	5	120	59.4	49.3	60.50	50.97
43	0.7	0.2	0.3	3	60	37.7	19.6	36.26	21.13
44	0.7	0.7	0.3	7	60	47.2	40.1	48.54	40.20
45	0.7	0.7	0.9	7	60	56.7	42.1	57.59	42.14
46	0.7	0.2	0.9	3	180	49.1	27.6	49.12	29.12

Table 2 (continued)

Run	Input factors					Experimental		RSM-predicted	
	A: TiO ₂ (g/L)	B: ZnO (g/L)	C: H ₂ O ₂ (mL/L)	D: pH	E: RT (min)	TOC removal (%)	COD removal(%)	TOC removal (%)	COD removal (%)
47	0.7	0.7	0.9	7	180	67.1	47.1	65.68	48.20
48	0.45	0.45	0.6	5	120	61.7	51.4	60.50	50.97

Table 3 Analysis of variance (ANOVA) results of second-order models for TOC removal

Source	Sum of squares	df	Mean square	F value	p value		
<i>Model</i>	5067.84	9	563.09	209.22	<0.0001	Significant	
A—TiO ₂	517.92	1	517.92	192.43	<0.0001		
B—ZnO	15.83	1	15.83	5.88	0.0202	Mean	50.23
C—H ₂ O ₂	597.24	1	597.24	221.91	<0.0001	R ²	0.9768
D—pH	1449.53	1	1449.53	538.57	<0.0001	Adj. R ²	0.9568
E—RT	556.07	1	556.07	206.61	<0.0001	Pred. R ²	0.9282
AC	17.26	1	17.26	6.41	0.0156	SD	1.64
CD	36.77	1	36.77	13.66	0.0007	CV %	3.27
A ²	201.20	1	201.20	74.76	<0.0001	Adeq. Prec.	53.4
B ²	177.72	1	177.72	66.03	<0.0001		
<i>Residual</i>	102.27	38	2.69				
Lack of fit	85.30	33	2.58	0.7615	0.7175	Not significant	
Pure error	16.97	5	3.39				
Cor total	5170.11	47					

Table 4 Analysis of variance (ANOVA) results of second-order models for COD removal

Source	Sum of squares	df	Mean square	F value	p value		
<i>Model</i>	6020.87	11	547.35	322.71	<0.0001	Significant	
A—TiO ₂	717.60	1	717.60	423.08	<0.0001		
B—ZnO	445.69	1	445.69	262.77	<0.0001	Mean	36.16
C—H ₂ O ₂	97.92	1	97.92	57.73	<0.0001	R ²	0.9662
D—pH	666.18	1	666.18	392.77	<0.0001	Adj. R ²	0.9471
E—RT	312.03	1	312.03	183.96	<0.0001	Pred. R ²	0.9114
AB	71.10	1	71.10	41.92	<0.0001	SD	1.3
AC	16.97	1	16.97	10.00	0.0032	CV %	3.60
A ²	45.57	1	45.57	26.87	<0.0001	Adeq. Prec.	64.3
B ²	36.28	1	36.28	21.39	<0.0001		
C ²	148.05	1	148.05	87.29	<0.0001		
E ²	78.37	1	78.37	46.21	<0.0001		
<i>Residual</i>	61.06	36	1.70				
Lack of fit	36.13	31	1.17	0.2337	0.9955	Not significant	
Pure error	24.93	5	4.99				
Cor total	6081.93	47					

incomparable. Making inference about the relative effect between process variables is possible from *coded factors equations*. In the coded equation, the relative influence of the factors on response can be determined by comparing the factor coefficients.

Effects of process variables as three-dimensional response surfaces

Figure 4a shows the 3D response surface plots for COD removal (%) obtained by statistical analysis through

Table 5 Final ANOVA **regression model equations for COD and TOC responses in terms of actual and coded factors

	Coded factors equations	Actual factors equations
COD removal (%)	$= 50.97 + 4.59 \times A + 3.62 \times B + 1.70 \times C + 4.43 \times D + 3.03 \times E + 1.49 \times A \times B - 0.73 \times A \times C - 4.17 \times A^2 - 3.72 \times B^2 - 7.52 \times C^2 - 5.47 \times E^2$	$-59.72 + 73.58 \times \text{TiO}_2 + 57.38 \times \text{ZnO} + 110.35 \times \text{H}_2\text{O}_2 + 2.21 \times \text{pH} + 0.41 \times \text{RT} + 23.85 \times \text{TiO}_2 \times \text{ZnO} - 9.71 \times \text{TiO}_2 \times \text{H}_2\text{O}_2 - 66.79 \times \text{TiO}_2^2 - 59.59 \times \text{ZnO}^2 - 83.61 \times \text{H}_2\text{O}_2^2 - 0.001 \times \text{RT}^2$
TOC removal (%)	$= 60.5 + 3.9 \times A + 0.68 \times B + 4.19 \times C + 6.53 \times D + 4.04 \times E - 0.74 \times A \times C + 1.07 \times C \times D - 7.48 \times A^2 - 7.03 \times B^2$	$= -24.84 + 129.19 \times \text{TiO}_2 + 103.95 \times \text{ZnO} + 9.44 \times \text{H}_2\text{O}_2 + 2.19 \times \text{pH} + 0.067 \times \text{RT} - 9.79 \times \text{TiO}_2 \times \text{H}_2\text{O}_2 + 1.78 \times \text{H}_2\text{O}_2 \times \text{pH} - 119.67 \times \text{TiO}_2^2 - 112.47 \times \text{ZnO}^2$

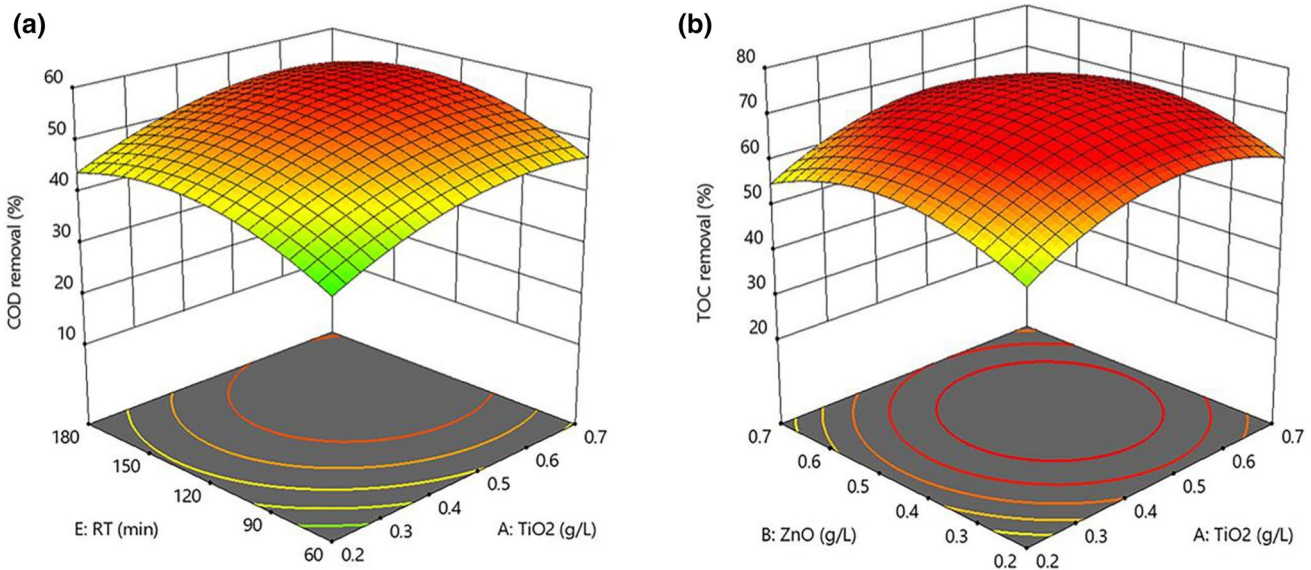


Fig. 4 **a** 3D plot for COD removal (%) versus reaction time (RT) and TiO_2 dosage at optimum settings of $\text{pH} = 7.0$, ZnO dosage = 0.502 g/L and H_2O_2 dosage = 0.745 mL/L . **b** 3D-plot for TOC removal (%)

versus ZnO (g/L) and TiO_2 (g/L) at optimum settings of H_2O_2 dose = 0.745 mL , $\text{pH} = 7$ and reaction time (RT) = 162.2 min

Design-Expert software. The plots demonstrate the effects of reaction time (RT) and TiO_2 dosage on the response when the other three variables kept constant at their optimum level (ZnO dosage = 0.502 g/L , $\text{pH} = 7$ and $\text{H}_2\text{O}_2 = 0.745 \text{ mL/L}$). The dome-shaped surface of the response indicates that the factor A: TiO_2 dosage and factor E: reaction time (RT) have a quadratic effect on COD removal. The second-order terms (A^2 and E^2) of the COD model in Table 5 validate this argument. The colour-coded optimum region (red) demonstrates that optimum COD removal is attained at TiO_2 dosage = 0.535 g/L and reaction time (RT) = 162 min .

Figure 4b demonstrates the RSM plot for TOC removal versus ZnO (g/L) and TiO_2 (g/L) at optimum settings of H_2O_2 dose = 0.745 mL , $\text{pH} = 7$ and reaction time (RT) = 162.2 min . The perfect dome-shaped surface indicates that the maximum TOC removal (%) is achieved near the centre values of both TiO_2 and ZnO factors. Optimum conditions from Table 6: TiO_2 dosage = 0.535 g/L , ZnO

dosage = 0.502 g/L indicate that colour-coded peak appears near to the centre of the design space. The quadratic effects of both TiO_2 and ZnO on TOC removal (%) is visible from the curvature of the response and also from the second-order terms of factors A and B in the coded equation of TOC removal (%) (Table 5). It is observed that the removal efficiency is decreasing at higher concentration of catalysts due to the turbidity factor, which impedes the passing of solar light for the photocatalytic reaction (Malato et al. 2009).

Synergistic effects of TiO_2 and ZnO dosages

The efficiency of the photocatalytic treatment process also depends on the ratio of TiO_2 and ZnO dosages used in each experimental runs. Both OFAT and RSM studies suggested that the concentration of the catalyst should be near to 1:1 proportions and higher dosages decline the amount of organic removal. Optimum catalysts dosage is necessary to avoid turbidity and opacity due to excess amount, hindering

Table 6 Optimum RSM and GA solutions for COD and TOC removal (%) efficiencies and experimental validation results

Optimization technique	Parameters	Optimum solution	Validation results	Optimum condition
RSM-DF optimization	COD removal (%)	55.55	51.2	TiO ₂ dosage = 0.535 g/L
	TOC removal (%)	72.58	68.6	ZnO dosage = 0.502 g/L, pH = 7
	Desirability	0.64		H ₂ O ₂ = 0.745 mL/L, RT = 162 min
GA optimization (Pareto optimal solution selected for validation)	COD removal (%)	63.9	61.2	TiO ₂ dosage = 0.51 g/L
	TOC removal (%)	76.5	73.3	ZnO dosage = 0.46 g/L, pH = 6.9
				H ₂ O ₂ = 0.89 mL/L, RT = 179 min

sunlight absorption during the photocatalytic process. The 'AB' interaction term between factors A: TiO₂ and B: ZnO present in the coded equation in Table 5 shows their combined effect on COD removal (%). The perfect dome-shaped curvature of response in Fig. 4b indicates that both the factors simultaneously increase the removal efficiency near to the centre of the design space and at extreme ranges (four corners, -1 and +1 levels) the removal is minimal. The synergistic effect in TiO₂-ZnO combination is due to the enrichment of charge transfer resulting in enhancement of hydroxyl radical production (Palominos et al. 2009). The second-order terms (A^2 and B^2) in both TOC and COD model show the quadratic effect of TiO₂ and ZnO on organic removal.

Even though due to catalyst dosage, a large number of active sites are generated, a limiting point is reached where the excessive amount resulting in turbidity reducing light penetration. The trade-off between these two competing phenomena decides the optimum catalysts dosage required for efficient photocatalytic degradation. In the present study, TiO₂ dosage of 0.51 g/L and ZnO dosage of 0.46 g/L (RSM-GA) were found to be optimum by achieving 61.2% removal of COD and 73.3% removal of TOC through validation experiments. Similar synergistic mineralisation performance was exhibited in a previous study where TOC removal efficiency (%) was reached up to 95.3% for simulated solar photocatalysis of methylene blue removal (at pH = 7) using TiO₂/ZnO/reduced graphene oxide composite (Nguyen et al. 2020). The results from the present study confirm that similar TOC and COD degradation of organic pollutants can be achieved at circumneutral pH of the seawater.

Effects of pH

The pH of the reaction mixture is a significant parameter in oxidation processes. Determining the most effective pH is still being debated widely because of the intermediates that were formed can result in different optimum pH values. In the current study, the optimum pH required for maximum TOC and COD degradation was found to be 6.9 (from RSM-GA optimization). Since adjusting a large volume of seawater pH to 6.9 in an RO desalination plant on a daily

basis is problematic, experimental runs were also conducted without changing the initial pH of seawater, which was 7.8 (average). From the confirmation run (which was conducted at RSM-GA optimum setting), comparable organics removal efficiencies (TOC removal = 66.4%, COD removal = 49.2%) were observed when seawater pH kept constant (as target pH = 8). At circumneutral pH, similar photocatalytic degradation efficiency was achieved in a previous study (Ji et al. 2017) where degradation rate of diesel pollutants from seawater was reached up to 87.74% using TiO₂/ZrO₂ catalysts under visible light. Also, it was reported that, for solar photocatalytic disinfection of water, the degradation efficiency does not depend significantly on pH at ranges from 4 to 10 (Malato et al. 2016).

The positive coefficients of factor D (pH) in the model equations (coded factors) given in Table 5, show that pH has a tendency towards the upper limit (which was set as 7) for improving organic removal efficiency. At pH less than optimal conditions, generation of 'OH radicals become comparatively lower and lead to reduced oxidation of organics. pH also affects the position of conductance and valance bands, size of catalyst agglomeration and the charge on catalyst particles. Increasing the pH above optimal condition results in a lower generation of H⁺ ions that further results in lower production of 'OH radicals (Jung et al. 2009). At acidic operational pH, the surface charge for TiO₂ becomes positive and exerts an attractive electrostatic force on anionic organic composites. Such polar attraction between negatively charged compounds and TiO₂ enhances adsorption rate for succeeding photocatalysis. The surface charge property of the catalyst alters with deviation in pH of the solution. The point of zero charge (PZC) for Degussa-P25-TiO₂ is around 6.8 (Gogniat et al. 2006). In basic solution, the TiO₂ surface is negatively charged, and when pH is lower than PZC, it is charged positively. The PZC value is altered when using TiO₂ catalyst with ZnO powder. Hence, in the current study, the optimum organic removal is achieved at near-neutral pH. Similar ranges of optimum values were reported by Kim et al. (2012) where they have demonstrated the synergistic effect of two different advanced oxidation processes (TiO₂ and Fenton-like reaction) resulted

in enhanced $\cdot\text{OH}$ production and drastic improvement in the oxidation of organic pollutant at circumneutral pH values.

Effect of H_2O_2

The influence of hydrogen peroxide on the organic removal efficiency was investigated in the range of 0.2–1.0 mL/L. The optimum dosage of H_2O_2 (= 0.89 mL/L, from RSM-GA optimization) and the positive coefficients of factor C (H_2O_2) in the coded equations for TOC and COD removal (%) as given in Table 5 indicate its positive influence on overall organics degradation. This is attributed to the ability of H_2O_2 for scavenging electron and enhancing the production of hydroxyl radicals (Jamil et al. 2019). Apart from preventing charge recombination, by accepting electrons, oxidants like H_2O_2 may dissociate into highly reactive radicals and thereby improve the mineralization efficiency (Diya'Uddein et al. 2011). Oxidative degradation of organics is enhanced at the higher concentration of hydrogen peroxide leading to an overall increase in TOC and COD removal from the seawater.

Effect of irradiation time

Irradiation time has a significant role in decontamination of polluted water through heterogeneous photocatalysis. Irradiation time depends on the initial concentration and ionic state of various organic contaminants present in seawater as well as the type of catalyst used. Since seawater is very complex, it is not easy to degrade some contaminants into water and CO_2 . In the present study, the optimum irradiation time obtained from RSM-DF and RSM-GA simulation studies was 162 min and 179 min, respectively. The optimum reaction time in this study is very less when compared with a previous photocatalytic degradation study (Zulfiqar et al. 2019), where the irradiation time was 540 min for optimum removal of phenol using TiO_2 nanocatalysts. When compared with photocatalytic degradation of other industrial effluents, the irradiation time is significantly less in seawater treatment if the reaction is performed under optimum conditions. Factors such as photonic flux absorbed by TiO_2/ZnO , uniform distribution of catalysts in suspension, continuous flow of seawater through borosilicate tubular reactor contribute to achieve faster degradation of organics. The availability of high solar irradiance in the region (670 Watts/m^2) also enhanced the overall degradation rate.

Process optimization using response surface methodology (RSM) and desirability function (DF)

In RSM, desirability function (DF) is used to optimize multiple responses in order to achieve maximal removal efficiencies of TOC and COD simultaneously. This

approach enables to locate the optimal settings of the variables to attain the desired response. According to the numerical optimization steps in the Design-Expert (version 11) software, the desired goal for input variables (TiO_2 , ZnO , H_2O_2 dosages, pH and RT) is chosen as “in range”, while TOC and COD removal (%) responses are defined as “maximum”. The software combines the individual desirability to determine the best set of trade-offs. The programme then searches the design space to optimize desirability function based on the defined goals. Table 6 shows the values of optimum removal efficiencies forecasted by the model under optimum process operating conditions. Additional experiments were performed to confirm the validity of the prediction, revealing agreement between predicted and experimental results.

The TOC and COD percentage degradation obtained from RSM-DF analysis was found to be more than that resulted from OFAT analysis (72.58% and 55.55% against 49.5% and 41.5%). This result shows that the study on interaction or interdependence of influencing factors is critical in a multivariate system. The synergistic or antagonistic effects of input factors on responses are not visible in the univariate investigation of OFAT analysis of any process. Solar photocatalytic seawater treatment is a complex multivariate process in which the system performance and organic removal efficiency are affected by a large number of synergistic and antagonistic interactions and main effects. While OFAT is suitable for screening and range finding, RSM provides more insight into the process behaviour.

Genetic algorithm (GA) multiobjective optimization

While RSM uses the desirability function (DF) approach for optimization, the genetic algorithm utilizes adaptive heuristic search techniques based on evolutionary ideas of genetics and natural selection (Bhatti et al. 2011). In complex processes like seawater solar photocatalysis, finding the global optima is cumbersome with conventional techniques as more often the solution tends to converge to local minima or maxima. Many technicals have found the superiority of GA over other optimization techniques as the GA solutions are always better due to convergence to global optimum (Betiku et al. 2016; Gou et al. 2018). In the current study, the optimization capacity of RSM-desirability function (RSM-DF) technique is compared with the solutions generated by GA multiobjective optimization. The TOC and COD removal models developed using RSM were implemented in an optimization process using *gamultiobj* solver, one of the multiobjective optimizers included in MATLAB[®](2017a) software. The GA solver stochastically searches through the domain space to attain the optimum solution. GA is an optimization technique developed based on the principle of natural evolution (Yasin et al. 2014). The GA strategy starts

with the initialization of population known as chromosomes followed by fitness evaluation based on an objective function. The genetic propagation of chromosomes is based on the selection of the fittest and then through operators like crossover and mutation.

The five photocatalytic process factors which represent the input space of TOC and COD models (Table 2), were optimized using GA multiobjective solver from the optimization toolbox. This was attained through searching for the optimum solution that results in maximum removals of TOC and COD simultaneously. The RSM models of TOC and COD, developed in terms of actual factors (Table 5), were used as the fitness (objective) functions to evaluate the quality of the individual solution from the population. In terms of the GA toolbox implementation, the population type was selected as a double vector with crossover probability set as 0.9. The adaptive-feasible mutation was utilized to create genetic diversity and enable GA to search for broader space. The population size, function tolerance and the maximum number of generations were set at 100, 0.0001 and 100, respectively. Finally, the optimal results were derived as a fully converged Pareto front.

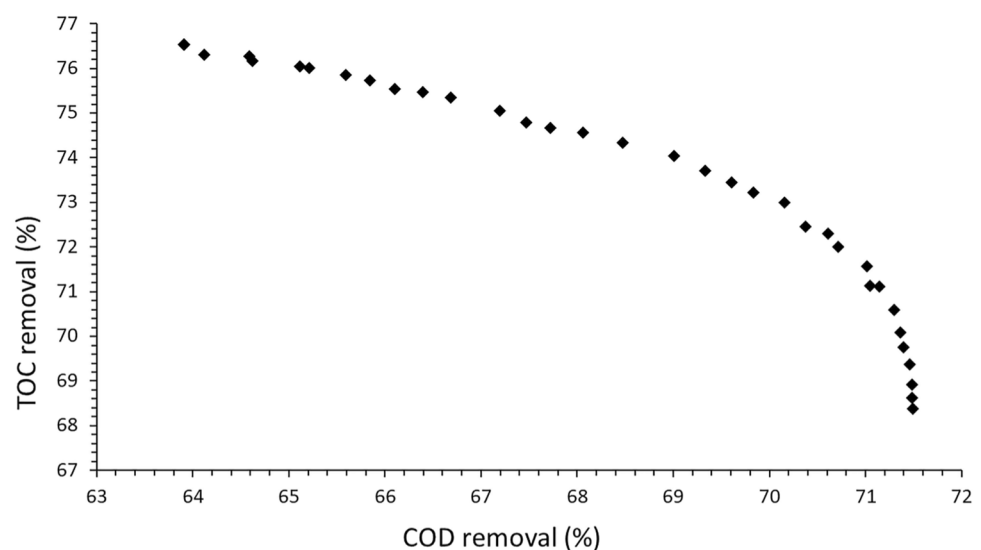
The Pareto front (Fig. 5) generated by *gamultiobj* solver, demonstrates the trade-off between two competing objectives (TOC and COD removal) and determines the non-dominated solutions. It includes those population members for which no other solution exists which is dominant than the Pareto set member. The GA optimizer in MATLAB® GA toolbox is essentially a minimization tool. Hence, the TOC and COD models (actual factors equations-Table 5) were negated when used as the objective function (fitness function). As depicted by the number of solution points in Fig. 5, the Pareto front gives a set of optimal solutions. Each point on the Pareto front is associated with a set of process factors (decision variables). In the current study, a

set of 36 solutions were generated as optimal on the Pareto set. From Pareto optimal sets, one solution with maximum TOC removal (73.3%) was selected for validation, and the results are shown in Table 6. The degradation efficiency could be improved by using doped nanophotocatalysts (with metals or non-metals) to reduce the bandgap energy and thereby enabling the reaction in the visible region of the solar spectrum. When compared to RSM-DF optimization, GA multiobjective solutions identify more accurate TOC and COD removal efficiencies under different optimum conditions. The closeness of validation results to the optimum results of GA (Table 6), supports the superiority of RSM-GA over RSM-DF method of optimization.

Conclusion

In this advanced oxidation treatment study, efficiency and performance evaluation for TOC and COD removal from seawater have been investigated. Main effects and interaction among crucial process factors such as TiO₂ dosage, H₂O₂ dosage, pH, reaction time (RT) and ZnO dosage were assessed to evaluate optimum operational settings and treatment efficiency. Process optimization and performance evaluation were undertaken using response surface methodology-desirability function (RSM-DF) and RSM integrated with genetic algorithm (RSM-GA) approaches. In RSM-DF method, organic removal, with a reaction time (RT) of 162 min, pH 7.0, TiO₂ dosage of 0.535 g/L, ZnO dosage of 0.502 g/L and H₂O₂ dosage of 0.745 mL/L was found to be optimum by achieving 55.55% of COD removal and 72.58% of TOC removal. The obtained optimum values using RSM-GA include a reaction time of 179 min, 0.51 g/L of TiO₂, 0.46 g/L of ZnO, pH 6.9 and 0.89 mL/L of H₂O₂. RSM-GA method gave higher organic removal rate at optimum

Fig. 5 Pareto-optimal set of solutions computed for multi-objective optimization of TOC removal efficiency (Objective-1) and COD removal efficiency (Objective-2)



conditions different from RSM-DF (COD removal = 63.9% and TOC removal = 76.5%). The results validate the performance of the multiobjective genetic algorithm for its convergence to the global optimum. The predicted RSM-GA results correspond well with the experimental results (COD removal = 61.2% and TOC removal = 73.3%). The synergistic removal efficiency obtained in this work demonstrates that the combination of TiO_2 catalyst with ZnO and H_2O_2 can be a feasible alternative for persistent organic removal. Thus, the solar mediated photocatalytic pretreatment of seawater can be applied as a sustainable technique for degradation of organics that foul RO membranes. The solar nanophotocatalysis of $\text{TiO}_2/\text{ZnO}/\text{H}_2\text{O}_2$ is a competitive method for decontaminating highly saline seawater by utilizing efficient renewable resources. Utilization of renewable solar energy coupled with optimum use of nanophotocatalysts enables this technique to be a unique treatment process for seawater reverse osmosis pretreatment and membrane fouling mitigation.

Funding The present work was not funded by any funding agency.

Compliance with ethical standards

Conflict of interest The authors declare that they have no conflict of interest.

Open Access This article is licensed under a Creative Commons Attribution 4.0 International License, which permits use, sharing, adaptation, distribution and reproduction in any medium or format, as long as you give appropriate credit to the original author(s) and the source, provide a link to the Creative Commons licence, and indicate if changes were made. The images or other third party material in this article are included in the article's Creative Commons licence, unless indicated otherwise in a credit line to the material. If material is not included in the article's Creative Commons licence and your intended use is not permitted by statutory regulation or exceeds the permitted use, you will need to obtain permission directly from the copyright holder. To view a copy of this licence, visit <http://creativecommons.org/licenses/by/4.0/>.

References

- Ab Aziz NA, Palaniandy P, Aziz HA, Dahlan I (2016) Review of the mechanism and operational factors influencing the degradation process of contaminants in heterogenous photocatalysis. *J Chem Res* 40:704–712. <https://doi.org/10.3184/174751916X14769685673665>
- Abdollahi H, Noaparast M, Ziaedin S et al (2019) Prediction and optimization studies for bioleaching of molybdenite concentrate using artificial neural networks and genetic algorithm. *Miner Eng* 130:24–35. <https://doi.org/10.1016/j.mineng.2018.10.008>
- Aljuboury DADA, Palaniandy P, Aziz HBA, Feroz S (2015) Treatment of petroleum wastewater using combination of solar photo-two catalyst TiO_2 and photo-Fenton process. *J Environ Chem Eng* 3:1117–1124. <https://doi.org/10.1016/j.jece.2015.04.012>
- Aljuboury DADA, Palaniandy P, Aziz HBA et al (2016) Evaluating photo-degradation of COD and TOC in petroleum refinery wastewater by using TiO_2/ZnO photo-catalyst. *Water Sci Technol* 74:1312–1325. <https://doi.org/10.2166/wst.2016.293>
- Amy G, Ghaffour N, Li Z et al (2017) Membrane-based seawater desalination: present and future prospects. *Desalination* 401:16–21. <https://doi.org/10.1016/j.desal.2016.10.002>
- Azevedo EB, Tôrres AR, Aquino Neto FR, Dezotti M (2009) TiO_2 -photocatalyzed degradation of phenol in saline media in an annular reactor: hydrodynamics, lumped kinetics, intermediates, and acute toxicity. *Braz J Chem Eng* 26:75–87. <https://doi.org/10.1016/j.apcatb.2004.06.014>
- Betiku E, Odude VO, Ishola NB et al (2016) Predictive capability evaluation of RSM, ANFIS and ANN: a case of reduction of high free fatty acid of palm kernel oil via esterification process. *Energy Convers Manag* 124:219–230. <https://doi.org/10.1016/j.enconman.2016.07.030>
- Bhatti MS, Kapoor D, Kalia RK et al (2011) RSM and ANN modeling for electrocoagulation of copper from simulated wastewater: multi objective optimization using genetic algorithm approach. *Desalination* 274:74–80. <https://doi.org/10.1016/j.desal.2011.01.083>
- Chatterjee S, Kumar A, Basu S, Dutta S (2012) Application of Response Surface Methodology for Methylene Blue dye removal from aqueous solution using low cost adsorbent. *Chem Eng J* 181–182:289–299. <https://doi.org/10.1016/j.cej.2011.11.081>
- Desai KM, Survase SA, Saudagar PS et al (2008) Comparison of artificial neural network (ANN) and response surface methodology (RSM) in fermentation media optimization: case study of fermentative production of scleroglucan. *Biochem Eng J* 41:266–273. <https://doi.org/10.1016/j.bej.2008.05.009>
- Dibaba OR, Lahiri SK, T'Jonck S, Dutta A (2016) Experimental and artificial neural network modeling of a Upflow Anaerobic Contactor (UAC) for biogas production from Vinasse. *Int J Chem React Eng* 14:1241–1254. <https://doi.org/10.1515/ijcre-2016-0025>
- Diya'Uddein BH, Daud WMAW, Abdul Aziz AR (2011) Treatment technologies for petroleum refinery effluents: a review. *Process Saf Environ Prot* 89:95–105. <https://doi.org/10.1016/j.psep.2010.11.003>
- Gogniat G, Thyssen M, Denis M, Pulgarin C, Dukan S (2006) The bactericidal effect of TiO_2 photocatalysis involves adsorption onto catalyst and the loss of membrane integrity. *FEMS Microbiol Lett* 258:18–24
- Gou S, Nik VM, Scartezzini JL et al (2018) Passive design optimization of newly-built residential buildings in Shanghai for improving indoor thermal comfort while reducing building energy demand. *Energy Build* 169:484–506. <https://doi.org/10.1016/j.enbuid.2017.09.095>
- Hassani A, Khataee A, Fathinia M, Karaca S (2018) Photocatalytic ozonation of ciprofloxacin from aqueous solution using TiO_2/MMT nanocomposite: nonlinear modeling and optimization of the process via artificial neural network integrated genetic algorithm. *Process Saf Environ Prot* 116:365–376. <https://doi.org/10.1016/j.psep.2018.03.013>
- Jamil A, Bokhari TH, Javed T et al (2019) Photocatalytic degradation of disperse dye Violet-26 using TiO_2 and ZnO nanomaterials and process variable optimization. *J Mater Res Technol*. <https://doi.org/10.1016/j.jmrt.2019.11.035>
- Ji Q, Yu X, Zhang J et al (2017) Photocatalytic degradation of diesel pollutants in seawater by using ZrO_2 (Er 3+)/ TiO_2 under visible light. *J Environ Chem Eng* 5:1423–1428. <https://doi.org/10.1016/j.jece.2017.01.011>
- Jiménez S, Micó MM, Arnaldos M et al (2017) Treatment of cleaning waters from seawater desalination reverse osmosis membranes for reutilization purposes. Part II: application of photo-Fenton and photocatalysis processes. *J Water Process Eng* 19:283–290. <https://doi.org/10.1016/j.jwpe.2017.08.008>

- Jung YS, Lim WT, Park JY, Kim YH (2009) Effect of pH on Fenton and Fenton-like oxidation. *J Environ Technol* 30:183–190
- Kaneva N, Bojinova A, Papazova K, Dimitrov D (2015) Photocatalytic purification of dye contaminated sea water by lanthanide (La^{3+} , Ce^{3+} , Eu^{3+}) modified ZnO. *Catal Today* 252:113–119. <https://doi.org/10.1016/j.cattod.2014.12.008>
- Khedr MG (2011) Membrane fouling problems in reverse osmosis desalination plants. *Desalin Water Reuse* 10:8–17
- Kim HE, Lee J, Lee H, Lee C (2012) Synergistic effects of TiO_2 photocatalysis in combination with Fenton-like reactions on oxidation of organic compounds at circumneutral pH. *Appl Catal B Environ* 115–116:219–224. <https://doi.org/10.1016/j.apcatb.2011.12.027>
- Kumar A, Kumar V (2019) Modeling and optimization of fixed mode dual effect (photocatalysis and photo-Fenton) assisted Metronidazole degradation using ANN coupled with genetic algorithm. *J Environ Manag.* <https://doi.org/10.1016/j.jenvman.2019.109428>
- Malato S, Fernández-Ibáñez P, Maldonado MI et al (2009) Decontamination and disinfection of water by solar photocatalysis: recent overview and trends. *Catal Today* 147:1–59. <https://doi.org/10.1016/j.cattod.2009.06.018>
- Malato S, Maldonado MI, Fernández-Ibáñez P et al (2016) Decontamination and disinfection of water by solar photocatalysis: the pilot plants of the Plataforma Solar de Almeria. *Mater Sci Semicond Process* 42:15–23. <https://doi.org/10.1016/j.mssp.2015.07.017>
- Matin A, Khan Z, Zaidi SMJ, Boyce MC (2011) Biofouling in reverse osmosis membranes for seawater desalination: phenomena and prevention. *Desalination* 281:1–16. <https://doi.org/10.1016/j.desal.2011.06.063>
- Mukherjee R, Chakraborty R, Dutta A (2019) Comparison of optimization approaches (response surface methodology and artificial neural network-genetic algorithm) for a novel mixed culture approach in soybean meal fermentation. *J Food Process Eng* 42:1–10. <https://doi.org/10.1111/jfpe.13124>
- Nguyen CH, Tran ML, Van Tran TT, Juang RS (2020) Enhanced removal of various dyes from aqueous solutions by UV and simulated solar photocatalysis over $\text{TiO}_2/\text{ZnO}/\text{rGO}$ composites. *Sep Purif Technol.* <https://doi.org/10.1016/j.seppur.2019.115962>
- Palominos RA, Mondaca MA, Giraldo A et al (2009) Photocatalytic oxidation of the antibiotic tetracycline on TiO_2 and ZnO suspensions. *Catal Today* 144:100–105. <https://doi.org/10.1016/j.cattod.2008.12.031>
- Rubio D, Casanueva JF, Nebot E (2013) Improving UV seawater disinfection with immobilized TiO_2 : study of the viability of photocatalysis ($\text{UV254}/\text{TiO}_2$) as seawater disinfection technology. *J Photochem Photobiol A Chem* 271:16–23. <https://doi.org/10.1016/j.jphotochem.2013.08.002>
- Sen S, Dutta S, Guhathakurata S et al (2017) Removal of Cr(VI) using a cyanobacterial consortium and assessment of biofuel production. *Int Biodeterior Biodegrad* 119:211–224. <https://doi.org/10.1016/j.ibiod.2016.10.050>
- Sharma N, Khanna R, Singh G, Kumar V (2017) Fabrication of 6061 aluminum alloy reinforced with $\text{Si}_3\text{N}_4/\text{n-Gr}$ and its wear performance optimization using integrated RSM-GA. *Part Sci Technol* 35:731–741. <https://doi.org/10.1080/02726351.2016.1196276>
- Tony MA, Zhao YQ, Purcell PJ, El-Sherbiny MF (2009) Evaluating the photo-catalytic application of Fenton's reagent augmented with TiO_2 and ZnO for the mineralization of an oil-water emulsion. *J Environ Sci Health Part A Toxic/Hazardous Subst Environ Eng* 44:488–493. <https://doi.org/10.1080/10934520902719894>
- Voutchkov Nikolay (2017) Pretreatment for reverse osmosis desalination. Elsevier, Amsterdam
- Weinrich L, LeChevallier M, Haas CN (2016) Contribution of assimilable organic carbon to biological fouling in seawater reverse osmosis membrane treatment. *Water Res* 101:203–213. <https://doi.org/10.1016/j.watres.2016.05.075>
- Yang T, Peng J, Zheng Y et al (2018) Enhanced photocatalytic ozonation degradation of organic pollutants by ZnO modified TiO_2 nanocomposites. *Appl Catal B Environ* 221:223–234. <https://doi.org/10.1016/j.apcatb.2017.09.025>
- Yasin Y, Ahmad FBH, Ghaffari-Moghaddam M, Khajeh M (2014) Application of a hybrid artificial neural network-genetic algorithm approach to optimize the lead ions removal from aqueous solutions using intercalated tartrate-Mg-Al layered double hydroxides. *Environ Nanotechnol Monit Manag* 1–2:2–7. <https://doi.org/10.1016/j.enmm.2014.03.001>
- Zulfiqar M, Samsudin MFR, Sufian S (2019) Modelling and optimization of photocatalytic degradation of phenol via TiO_2 nanoparticles: an insight into response surface methodology and artificial neural network. *J Photochem Photobiol A Chem* 384:112039. <https://doi.org/10.1016/j.jphotochem.2019.112039>

Publisher's Note Springer Nature remains neutral with regard to jurisdictional claims in published maps and institutional affiliations.